DOCKET NO. 50-249

File Copy (suppl.)
trans w/5-26-66 ltr

DRESDEN NUCLEAR POWER STATION

UNIT 3

PLANT DESIGN AND ANALYSIS REPORT

AMENDMENT NO. 3
ANSWERS TO AEC QUESTIONS

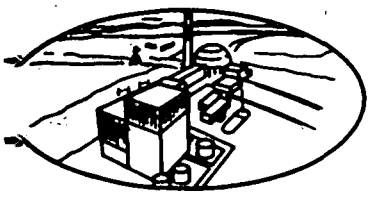

Commonwealth Edison Company

SUMMARY MEMORANDUM
ON
EXCURSION ANALYSIS UNCERTAINTIES

Prepared in response to questions by the
USAEC Division of Reactor Licensing

By

J. E. Boyden
H. A. Brammer
J. E. Wood

GENERAL ELECTRIC COMPANY
Atomic Power Equipment Department

May 23, 1966

FOREWORD

This Amendment Number 3 to the application for a construction permit and facility license for Unit 3 at the Dresden Nuclear Power Station, contains a Summary Memorandum on Excursion Analysis Uncertainties that has been prepared in response to various questions by the AEC Division of Reactor Licensing and the ACRS: Specifically in response to question Number 3 as requested by the Director, Division of Reactor Licensing, by letter to the Commonwealth Edison Company dated May 13, 1966.

As part of this amendment, pages V-3-24 and XI-2-7 are changed to record changes in the core spray cooling system. Revised pages V-3-24 and XI-2-7 are submitted.

SUMMARY MEMORANDUM ON EXCURSION ANALYSIS UNCERTAINTIES

I. INTRODUCTION

Recently a number of questions have arisen in AEC Staff and ACRS reviews regarding uncertainties in reactivity excursion analysis of General Electric Boiling Water Reactors. This document is a summary report of several studies relating to that subject. Of prime concern is the accuracy of estimating peak fuel enthalpy following a potential excursion, since this is used as an index of potential primary reactor system damage. Of equal importance is the estimated enthalpy limit or threshold at which such damage may be expected to occur. This report, then, addresses itself to the following areas:

a) Uncertainty in calculation of peak enthalpy.

b) Secondary reactivity effects which provide potential for additional energy release.

c) Uncertainty of damage threshold enthalpy limit.

II. SUMMARY AND CONCLUSIONS

In evaluating potential errors in reactivity excursion analyses, two distinct sources of uncertainty are evident. The first is statistical in nature, representing possible errors in experimental data and calculational inaccuracies. The second is a probabilistic uncertainty arising from the state variables of the reactor core.

Evaluation of statistical errors shows that an uncertainty of about 10 percent is associated with determination of peak fuel enthalpy.

Since a quantitative probabilistic analysis of excursion accidents is premature considering the present state of technology, all probabilistic variables are currently worst-cased. The sensitivity of peak fuel enthalpy to the probabilistic variables is much greater than for the statistical errors, so that a great deal of conservatism is introduced into the excursion analyses by this process.

Analysis of possible secondary reactivity effects has shown that potential sources of positive reactivity are small in magnitude and delayed sufficiently in time so as not to be significant to the course and consequences of reactivity excursions.

With respect to the threshold for potential primary system damage, studies have been made of fuel failure mechanisms which could possibly lead to rapid conversion of significant fission energy to mechanical energy. It has been estimated that the threshold for this process may occur at fuel enthalpies of approximately 425 calories per gram.

A review of the experimental data on fuel failure mechanisms has been very encouraging in that all of the available data tends to support the hypothesis developed from the fuel failure model predictions. There are some areas of uncertainty, however, where additional experimental data are needed in order to clarify the picture on fuel failure thresholds, particularly in the area of the effect of fission product gas release on prompt rupture thresholds for fully molten fuel.

No information available at the present time would lead to a change in the current position on fuel failure mechanisms or damage thresholds. Recognizing that uncertainties do exist in estimating the primary system damage threshold, however, a conservative design position of restricting credible excursions to peak enthalpies around the fuel melting range (220-280 cal/gm) has been adopted.

III. ANALYTICAL UNCERTAINTIES

This section briefly reviews the excursion calculational model, identifying variables with which errors may be associated. An uncertainty analysis discussion and summary then follows. In evaluating potential errors in the reactivity excursion calculation two distinct types of uncertainty are evident. The first is that arising from statistical errors in experimental data and calculations. The second is that associated with the conditional probability of the reactor being in some particular operating state at the time of the excursion and involves the state variables of the reactor core. For example, uncertainty in the experimental value of the Doppler coefficient reactivity feedback in the excursion calculation is statistical, while the spatial weighting factor, which multiplies the coefficient in the calculation, is geometry dependent and therefore probabilistic in nature. It is significant that the sensitivity of peak enthalpy to potential probabilistic uncertainties completely overwhelms the possible statistical errors.

Calculational Model

Analysis of the Doppler limited reactivity excursion accidents, described in numerous prior submittals, is performed by synthesizing spatial effects and the standard space-independent neutron kinetics calculation. Excursion initiating reactivity is introduced into the point kinetics calculation in time dependent format.

Doppler feedback to the kinetics calculation simulates a space-time kinetics analysis by means of a marching calculation. Initial neutron flux distributions associated with accidental reactivity addition are first determined utilizing a three-group, steady state diffusion calculation. A core averaged Doppler spatial weighting factor is determined from the flux distributions using perturbation theory techniques and utilized in the point kinetics equation to generate a small increment of power. In this case the kinetics calculation represents the average reactor condition.

This increment of power, expressed as a fuel temperature change, is then spatially distributed across the core according to initial flux distributions.

New spatially distributed cross sections are computed, reflecting the Doppler effect due to the added temperature, and another diffusion calculation is made. Comparison of the eigenvalue from this calculation to the eigenvalue resulting from a uniformly distributed temperature increment provides an accurate estimate of the change in Doppler weighting factor appropriate for the next kinetics calculational step. Utilizing this procedure the calculation is marched through to the termination of the excursion. Comparison of this procedure to a true space-time calculation[1] has shown virtually exact agreement for typical excursion transients.

Two conservative assumptions are introduced into the calculational procedure (as opposed to conservatism in input variables). First the excursion is assumed to be terminated only by Doppler reactivity feedback. Negative feedback from prompt moderator heating is conservatively ignored. Second, for design basis excursions, control rod scram is assumed to be actuated at 120% of rated power with a 0.2 second delay so that it is not effective in limiting the significant consequences of the excursion but only in holding the reactor subcritical well after Doppler has terminated the power burst. In actual operating practice scram trip is expected to be set within about a decade of actual power and in the more severe, low-power accidents may contribute to some extent in terminating the excursion.

The equations and variables used in excursion calculations are:

$$\frac{\partial P}{\partial t} = \left(\frac{\Delta k - \beta}{\ell^*}\right) P + \sum_{1}^{6} \lambda_i C_i \qquad (1)$$

$$\beta = \sum_{1}^{6} \beta_i \qquad (2)$$

$$\frac{\partial C_i}{\partial t} = \frac{\beta_i}{\ell^*} P - \lambda_i C_i \qquad 1 \leq i \leq 6 \qquad (3)$$

$$\Delta T = \frac{1}{C_p} \int_o^t P \, dt \qquad (4)$$

$$\Delta k_D = (DWF) \frac{N I_o \alpha}{\xi \Sigma s} \left(\sqrt{T_o + \Delta T} - \sqrt{T_o}\right) \qquad (5)[2]$$

$$\mathring{H} = H_o + (LPF)(P/A)(C_p \Delta T) \qquad (6)$$

where

P = reactor power

Δk = net reactivity - input less feedback

β = delayed neutron fraction

ℓ^* = prompt neutron lifetime

C_i = i^{th} fission product precursor concentration

λ_i = i^{th} fission product decay constant

T = fuel temperature

C_p = fuel specific heat

$N/\xi\Sigma s$ = resonance escape constants

I_o = base resonance integral

α = Doppler multiplier

Δk_D = Doppler reactivity feedback

DWF = spatial Doppler weighting factor

LPF = local power peaking factor

P/A = gross spatial peak-to-average power

H_o = base fuel enthalpy

$\hat{H}$ = peak fuel enthalpy

The variable $\hat{H}$ is the parameter which is used as the index of primary system damage.

Analysis of Statistical Uncertainties

Using a classical statistical approach assuming random independent variables, the uncertainty in $\hat{H}$ may be determined. If

$$\hat{H} = f(I_o, \alpha, \beta, \ldots) \qquad (7)$$

then the variance of $\hat{H}$ will be

$$\sigma^2(\hat{H}) = \sigma^2(I_o)\left(\frac{\partial f}{\partial I_o}\right)^2 + \sigma^2(\alpha)\left(\frac{\partial f}{\partial \alpha}\right)^2 + \sigma^2(\beta)\left(\frac{\partial f}{\partial \beta}\right)^2 + \cdots \qquad (8)$$

Table I lists the significant statistical variables, the estimated standard deviation of these variables and the contributions to the variance of $\hat{H}$. The standard deviation of the Doppler variables, I_o and α have been estimated from the data of Pettus[3] and Hellstrand[4][5]. These data for typical BWR fuel yields

	Pettus	Hellstrand
I_o	17.0	17.45
α	0.00653	0.00705

TABLE I

STATISTICAL UNCERTAINTIES IN EXCURSION ANALYSES

Parameter	Nominal Value	σ	$\sigma^2 \left(\frac{\Delta f}{\Delta \text{ Parameter}}\right)^2$
I_o	17.2	0.9	89
α	.0068	.0004	112
C_p	.08	.008	0
β	.0065	.001	0
ℓ^*	40×10^{-6}	4×10^{-6}	81
DWF	7.33	.36	78
P/A	20	1.6	2
LPF	1.3	.05	80

$\hat{H}$ = 211 cal/gm[2]

$\sigma^2 (\hat{H})$ = 442

$\sigma (\hat{H})$ = 21 cal/gm

The standard deviations in Table I were estimated about the nominal midpoint value of the two sets of data so as to include both data points and the estimated experimental uncertainty on each set of data.

On the variables C_p, β and ℓ^* it is convenient to include not only the statistical uncertainty in the estimated standard deviation, but also the probabilistic range that these variables assume with the reactor state conditions of temperature and fuel exposure. Table I, therefore, reflects the total uncertainty associated with these three variables.

The last three variables, DWF, P/A and LPF are predominantly state variables and, therefore, probabilistic in nature. They will be discussed further in the following section of this document. The standard deviations quoted in Table I, however, reflect the statistical calculational uncertainties, given a fixed reactor state. The DWF and P/A are not strictly statistically independent and extreme care is required in estimating calculational uncertainties. The DWF was calculated using first order, three-group perturbation theory at a variety of fixed power distributions. The results are shown in Figure 1 where DWF is plotted vs P/A. From this work it is estimated that the standard deviation in the calculation of DWF is approximately 5% of the DWF nominal value.

The results shown in Figure 1 are fit by the equation

$$\frac{P/A - 1}{DWF - 1} = 3 \qquad (9)$$

If these results are replotted in the form P/A ÷ DWF vs P/A, as shown in Figure 2, some information may be gained on the effect of statistical calculational errors in P/A. Peak fuel enthalpy, $\hat{H}$, is proportional to first order to the so-called damage parameter P/A ÷ DWF. For nominal values of P/A characteristic of excursions in large water reactors (e.g., 20), the sensitivity of $\hat{H}$ to errors in calculated P/A can be taken from Figure 2. Comparison of the excursion power distribution calculation to operating reactor data has indicated a standard deviation of about 8% in P/A. This leads to the variance of $\hat{H}$ shown in Table I.

It is noted that C_p and β contributions to the variance of $\hat{H}$ are nil. The variable β, of course, causes a proportional change in both input and feedback reactivity functions. The combined effect will change the width (time) of the excursion power burst slightly but the total area under the burst (enthalpy) is unchanged to first order.

The effect of the variable C_p is somewhat more subtle. The reactivity feedback loop in the kinetics calculation involving equations (1), (4) and (5) is actually independent of C_p, although the parameter appears in equation (4). This is evident if all the equations are converted to the dependent temperature variable, in which case C_p divides out of the system of equations. Therefore, from equation (6), $\hat{H}$ is directly proportional to C_p and to errors in C_p. However, significant parameters leading to fuel failure, such as UO_2 crystal growth, fuel melting point and particularly vapor pressure, are determined as functions of temperature. Conversion of these parameters to enthalpy damage limits also involves C_p directly. As

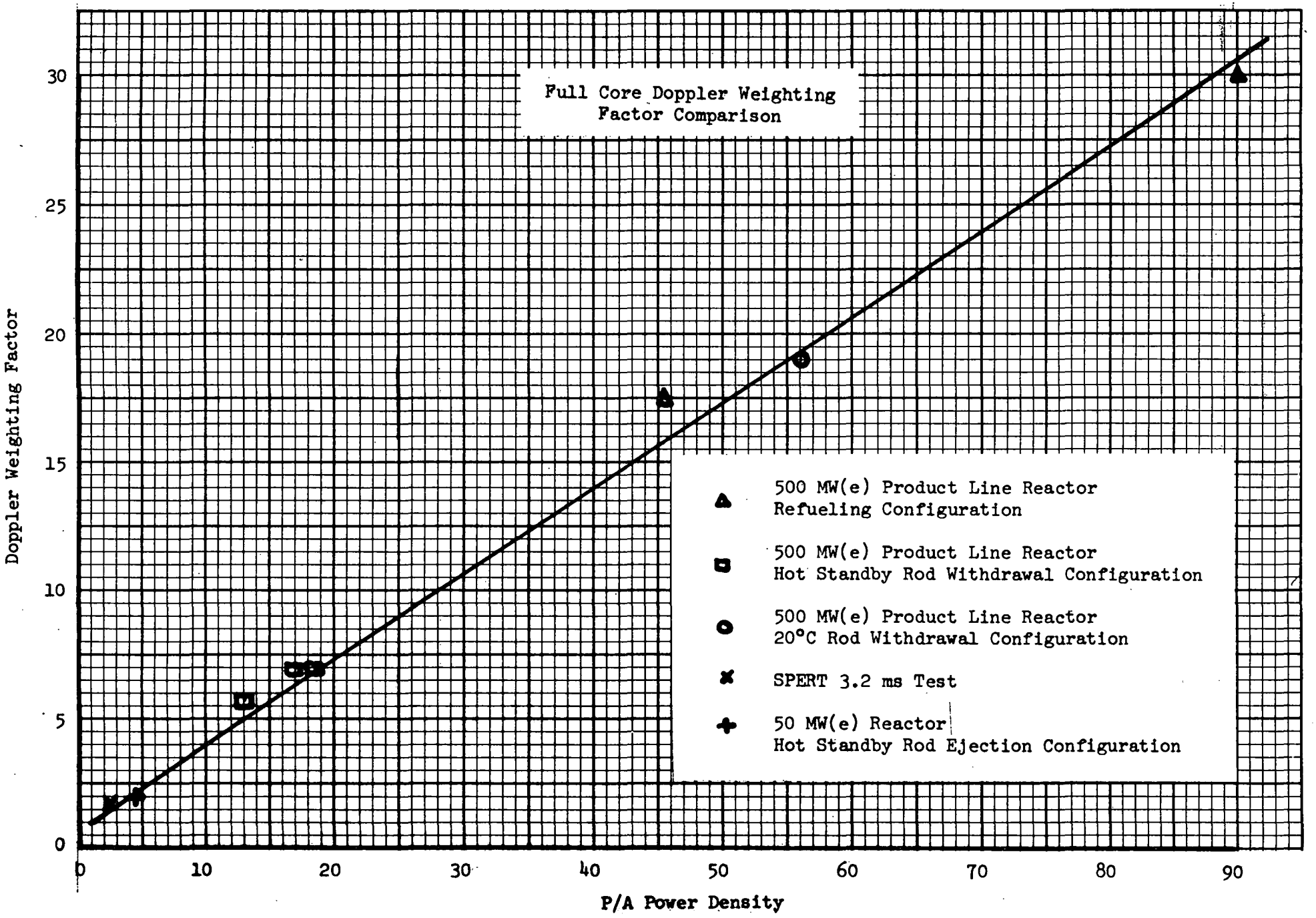
Full Core Doppler Weighting
Factor Comparison
Doppler Weighting Factor
P/A Power Density
0
5
10
15
20
25
30
0
10
20
30
40
50
60
70
80
90
500 MW(e) Product Line Reactor
Refueling Configuration
500 MW(e) Product Line Reactor
Hot Standby Rod Withdrawal Configuration
500 MW(e) Product Line Reactor
20°C Rod Withdrawal Configuration
SPERT 3.2 ms Test
50 MW(e) Reactor
Hot Standby Rod Ejection Configuration

Figure 1

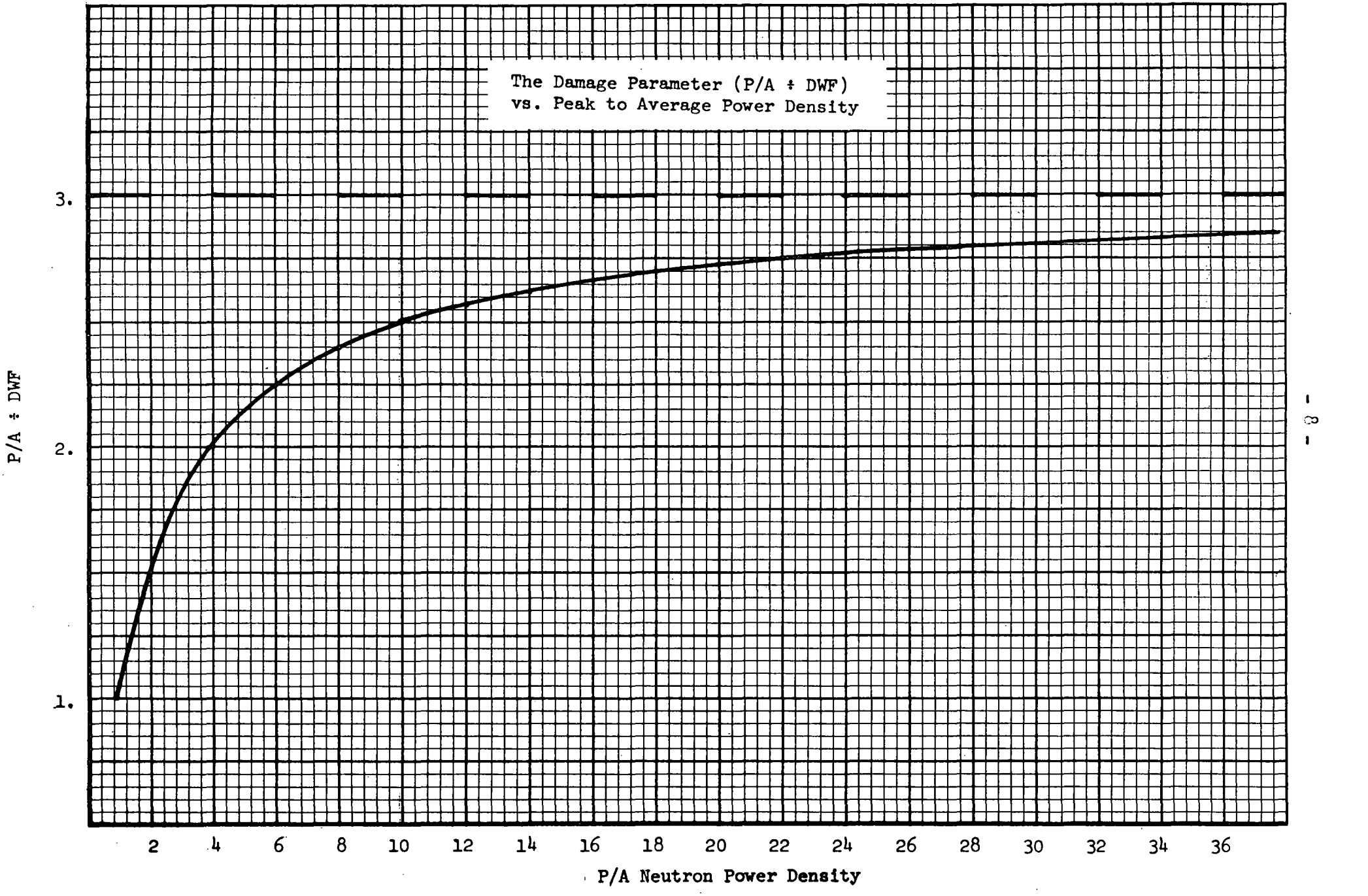
The Damage Parameter (P/A ÷ DWF)
vs. Peak to Average Power Density
P/A ÷ DWF
3.
2.
1.
2
4
6
8
10
12
14
16
18
20
22
24
26
28
30
32
34
36
P/A Neutron Power Density

Figure 2

long as C_p is used consistently in all these determinations there is no relative error introduced by this parameter between calculated $\hat{H}$, fuel melting damage and sudden fuel rupture limits.

Nominal values of the several reactor state parameters in Table I are specifically for a hot-standby reactor excursion. For this case the $\hat{H}$ = 211 cal/gm with an uncertainty of $\sigma(\hat{H}) = \pm 21$ cal/gm or about a 10% error. The statistical uncertainties on the parameters are virtually state independent and will, to first order, affect the variance of $\hat{H}$ relatively the same at other reactor states. Therefore, it may be concluded that the statistical uncertainty in $\hat{H}$ will be about 10% for all design basis accidents.

Analysis of Probabilistic Uncertainties

In addition to the statistical uncertainties discussed in the previous section, each variable in Table I, the reactivity input to equation (1) and the initial condition of equation (4) also vary across some determinable range with operating state of the reactor. The state of the reactor at the instant of a potential excursion is probabilistic, however. The true consequences of an excursion, therefore, depend on the conditional probability of a certain reactor state existing at the instant of the excursion. Significant pioneering work directed at this problem is now in progress[6]. In current BWR excursion analyses, however, the ultra-conservative approach of worst-casing all significant probabilistic variables is used. The conservatism introduced into the analyses by this process completely dominates any statistical error as covered in the previous section. Specifically the following conservatisms are used in the analysis.

Doppler parameters, I_o and α, used in the excursion calculation are characteristic of U-238 only. Over most of an operating reactor life a substantial inventory of Pu-240 exists which will contribute an estimated additional negative Doppler feedback of 10 to 15 percent[7]. This effect is ignored in the analysis. In addition a Doppler equation is utilized which lies below all measured data, and is more theoretically correct for extrapolation to elevated temperatures than either the Pettus or Hellstrand formulations. This is discussed in detail in the Appendix.

The probabilistic variation of C_p, β and ℓ^* has been included in the analysis shown in Table I.

The value of LPF used in the analysis is the highest expected in the life of the core. In particular, in exposed fuel containing high fission product inventory the LPF will be much depressed (by as much as 15 to 20 percent).

The DWF and P/A variables are conservatively chosen to yield the highest conceivable fuel enthalpy. From Figure 2 it is seen that the damage parameter, and fuel enthalpy, will be at a maximum if P/A is maximized. In geometrically modeling the excursion configurations, the initiating reactivity disturbance (such as a falling control rod) is assumed to occur in the center of the reactor with neutron flux radially peaked onto the rod to yield the proper rod worth. Further, as a control rod, for example, moves out of such a configuration there is a position at which axial peaking is greatest. It is always assumed that the prompt critical power burst

occurs at this point. The geometric assumptions, therefore, always yield the highest conceivable P/A and fuel enthalpy in each excursion analyzed.

Potential reactivity input to the excursion is also conservatively maximized. The reactivity input involves both reactivity worth of the initiating mechanism, such as a control rod, and its velocity. Typical sensitivity of peak enthalpy to these parameters for the case of a rod drop is shown in Figures 3 and 4. In this case control rod patterns are restricted, by engineered safeguards, to values generally below about 0.01 Δk. Early in core life, in very specific startup rod patterns, a few control rods may exist in the core with worths of about 0.025 Δk. This value, therefore is used in analyzing design basis excursions. Similarly, rod drop velocities are restricted by engineered safeguards to values below 5 feet per second. The analysis is performed, however, always using the maximum expected value of velocity.

Finally, the reactor power at the time of initiation of the excursion affects the rate of Doppler feedback through equation (4) and, therefore, is a significant probabilistic variable. Sensitivity of peak enthalpy to this parameter is shown in Figure 5. Here again the design basis accidents are conservatively analyzed using the lowest conceivable value of initial power as determined by the neutron source level in the reactor. It should be noted in passing that as the reactor approaches full power, significant increases in input reactivity rate can be tolerated with no change in excursion consequences. This is evident by comparing peak enthalpy variation between Figures 3, 4 and 5.

Comparison with SPERT Tests[8][9]

The final test of the overall validity of the excursion model would be a direct test against a variety of characteristic experiments. Unfortunately, only a few valid excursion experiments with UO_2 fueled assemblies exist. The tests most characteristic of BWR excursion analyses are the SPERT 3.2 ms and 1.55 ms experiments.

Analyses of these experiments with the BWR excursion model has shown agreement on all major parameters well within the accuracy of interpretation of the tests (estimated to be ~ 10%). Comparison with the 3.2 ms test, for example, is shown in Figure 6. These results tend to indicate that nothing of true significance has been overlooked in modeling the excursion analysis.

IV. SECONDARY REACTIVITY EFFECTS

Secondary reactivity effects may contribute to the course of excursions through the mechanism of moderator and fuel motion. Moderator heating and boiling during and following an excursion introduces negative reactivity feedback into the reaction kinetics and, as previously stated, is conservatively ignored.

Effects of potential fuel motion associated with design basis reactivity excursions have been reported in a prior submittal[10]. Potential for a

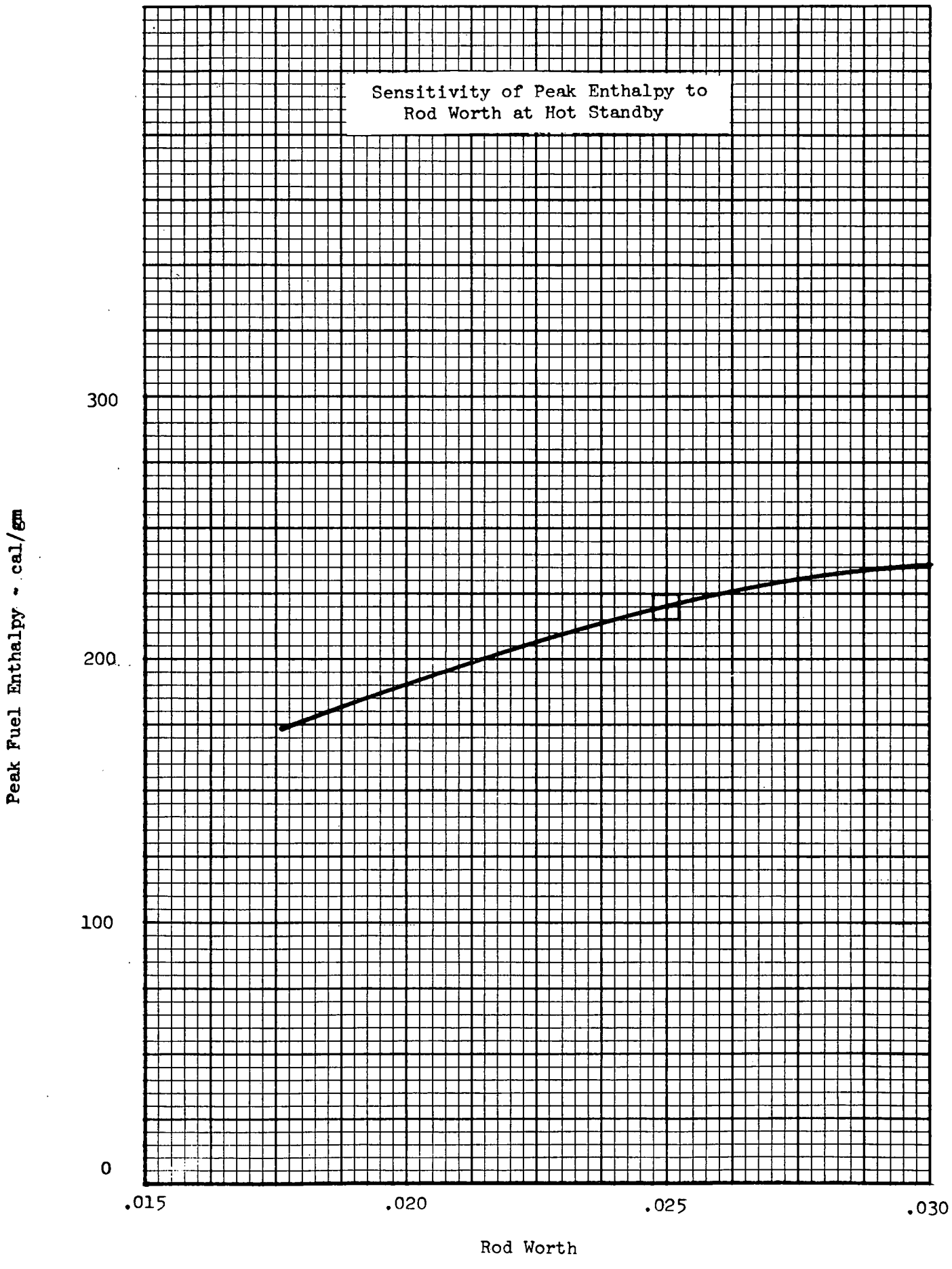
Sensitivity of Peak Enthalpy to
Rod Worth at Hot Standby
Peak Fuel Enthalpy - cal/gm
300
200
100
0
.015
.020
.025
.030
Rod Worth

Figure 3

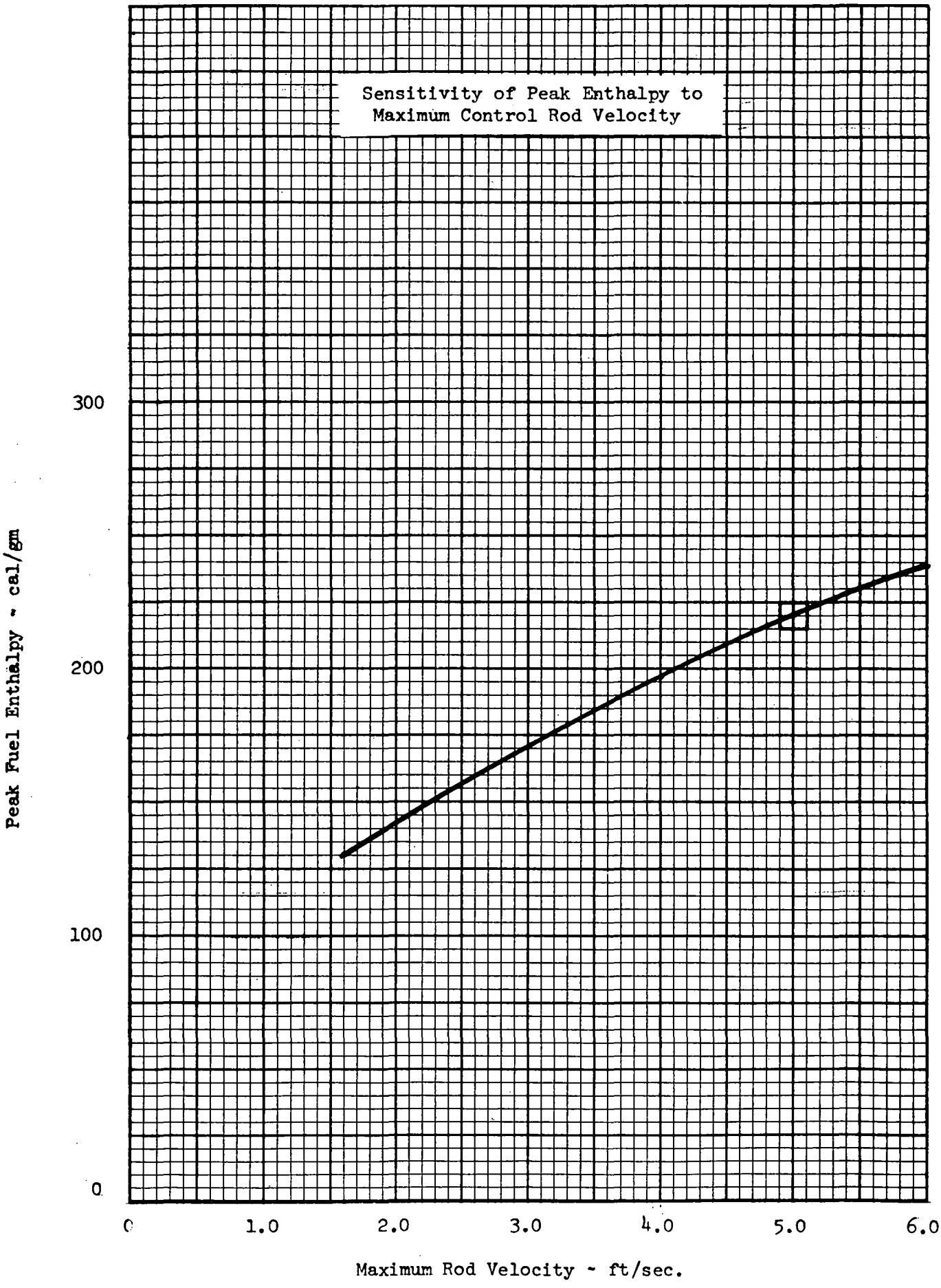
Sensitivity of Peak Enthalpy to
Maximum Control Rod Velocity
Peak Fuel Enthalpy - cal/gm
300
200
100
0
0
1.0
2.0
3.0
4.0
5.0
6.0
Maximum Rod Velocity - ft/sec.

Figure 4

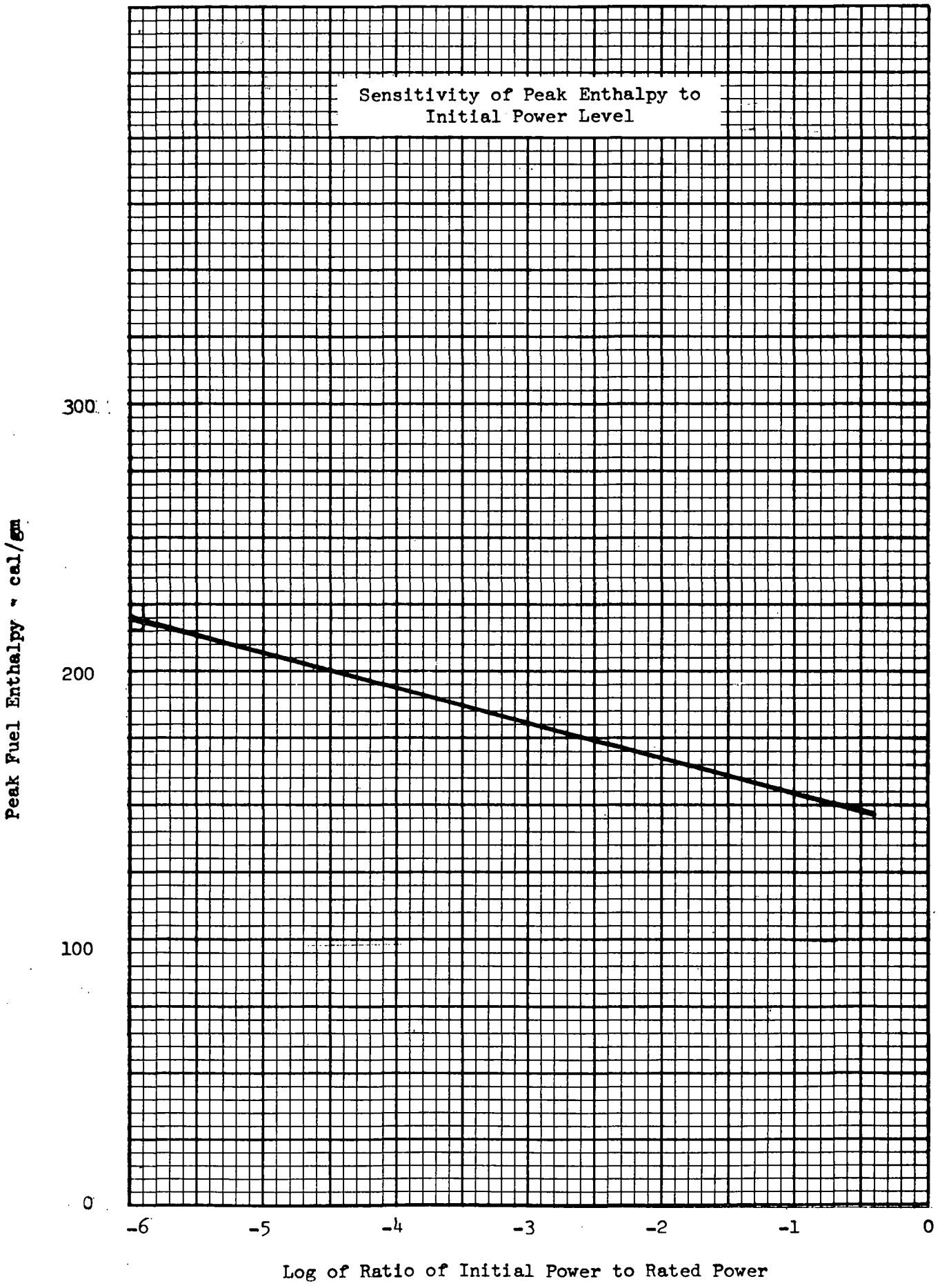
Sensitivity of Peak Enthalpy to
Initial Power Level
Peak Fuel Enthalpy - cal/gm
300
200
100
0
-6
-5
-4
-3
-2
-1
0
Log of Ratio of Initial Power to Rated Power

Figure 5

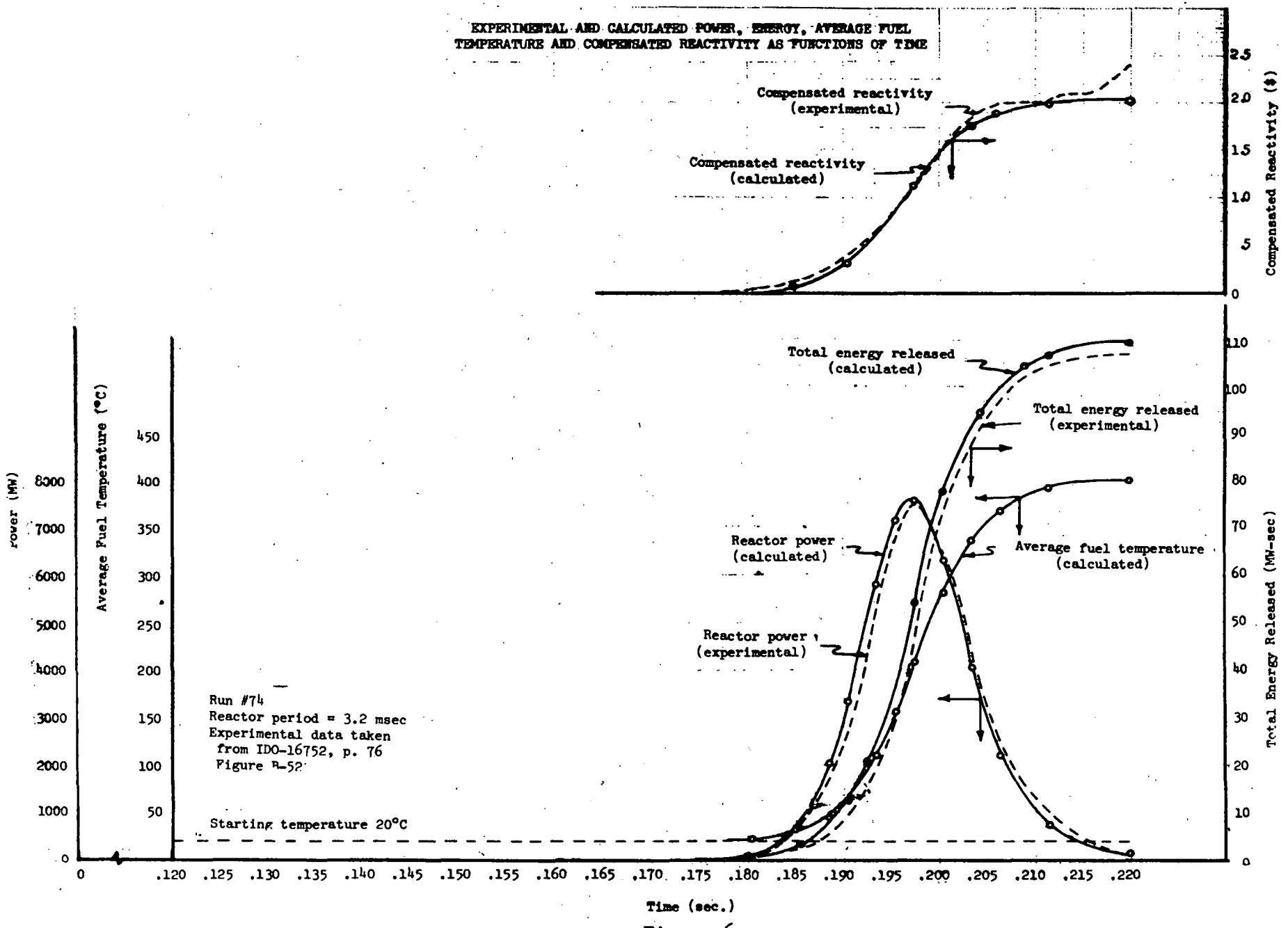
EXPERIMENTAL AND CALCULATED POWER, ENERGY, AVERAGE FUEL TEMPERATURE AND COMPENSATED REACTIVITY AS FUNCTIONS OF TIME
Compensated reactivity (experimental)
Compensated reactivity (calculated)
Compensated Reactivity ($)
Total energy released (calculated)
Total energy released (experimental)
Reactor power (calculated)
Reactor power (experimental)
Average fuel temperature (calculated)
Average Fuel Temperature (°C)
Total Energy Released (MW-sec)
Run #74
Reactor period = 3.2 msec
Experimental data taken from IDO-16752, p. 76 Figure B-52
Starting temperature 20°C
Time (sec.)

Figure 6

few cents of positive reactivity gain from fuel density increase exists upon fuel melting near the end of the excursion power burst. Since fuel slumping is involved, this reactivity gain is estimated to occur over a period of one second or longer.

Commencing at times approaching one second after the peak of the power burst, additional positive reactivity gains of a few tens of cents is conceivable.

Because of the small magnitudes and time delays associated with fuel motion, these effects are not significant to the course and consequences of the excursions. To further support this conclusion, several hypothetical analyses have been performed in which positive reactivity ramps were introduced at the peak of a rod drop excursion power burst. The conditions and results are shown in Table II. The calculated power bursts for Cases 58, 61 and 63 are shown in Figures 7 through 9.

TABLE II

SECONDARY REACTIVITY EFFECTS

Case	Δk Increment	Reactivity Rate	Peak Fuel Enghalpy, $\hat{H}$
63	0 - base case	-	220 cal/gm[2]
57	0.0025	0.005 Δk/sec	224
58	0.005	0.005	228
59	0.010	0.005	230
60	0.0025	0.030	240
61	0.005	0.030	244
62	0.010	0.030	255

As stated above, actual reactivity gains could potentially occur at the end, not at the peak, of the power burst. The lowest Δk increment included in Table II is approximately an order of magnitude larger than actual potential fuel motion effects. Further, the higher reactivity rates in the table are more than an order of magnitude greater than the maximum expected rates. Finally, negative moderator effects, which would be expected to exceed in magnitude any of the positive effects in the table, are ignored. Even under these extreme conditions no significant change, in terms of approaching primary system damage, is noted in the results.

An additional analysis, shown in Figure 10, in which a positive 0.015 Δk was introduced at 0.05 Δk/sec commencing at 0.5 second after the peak of the power burst indicates that positive reactivity effects delayed somewhat beyond the end of the initial power burst will not contribute to excursion consequences.

V. FUEL FAILURE MECHANISMS AND DAMAGE THRESHOLD

The reactivity excursion accident has been of major concern, primarily because of the potentially high rate of release of fission energy during

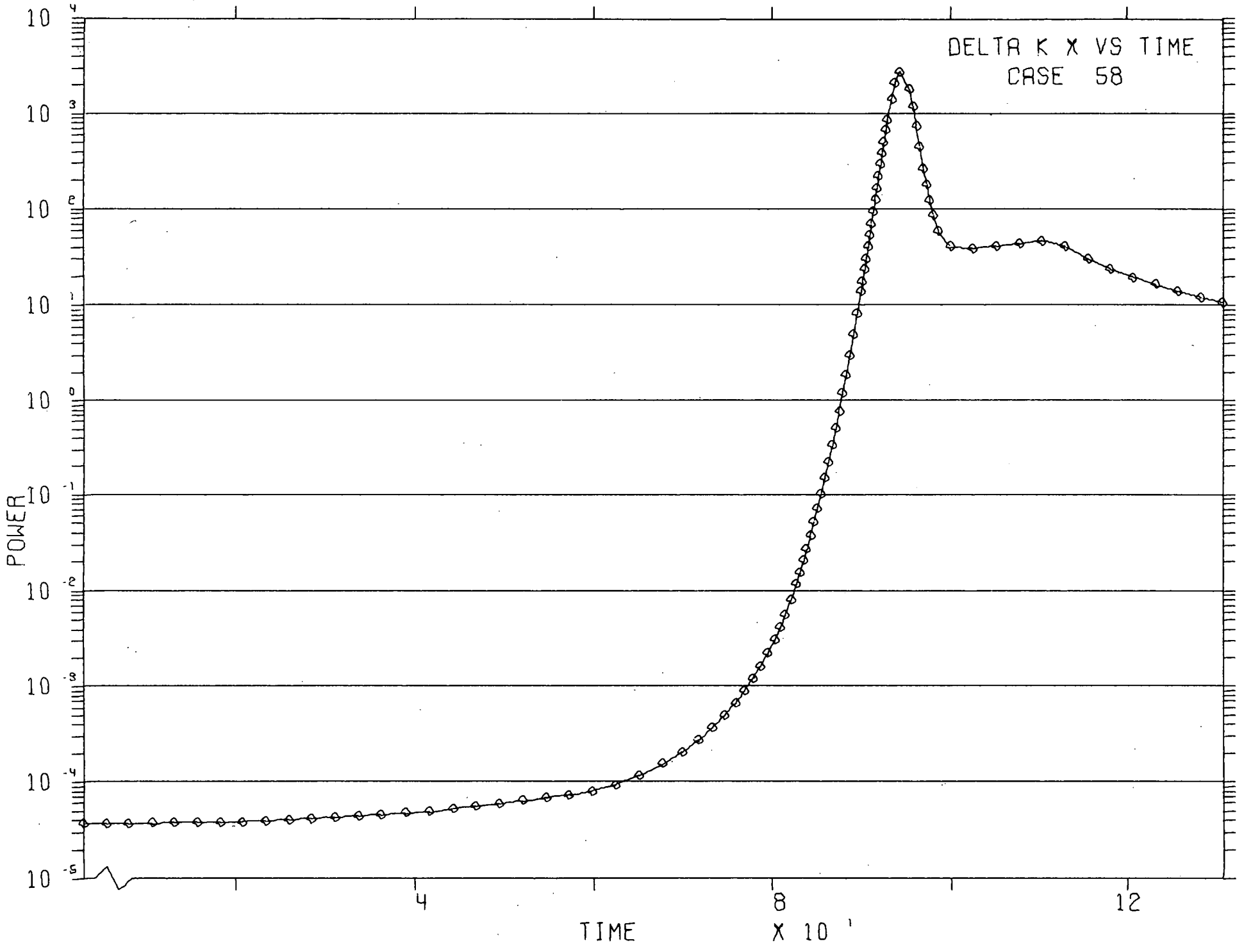

Figure 7

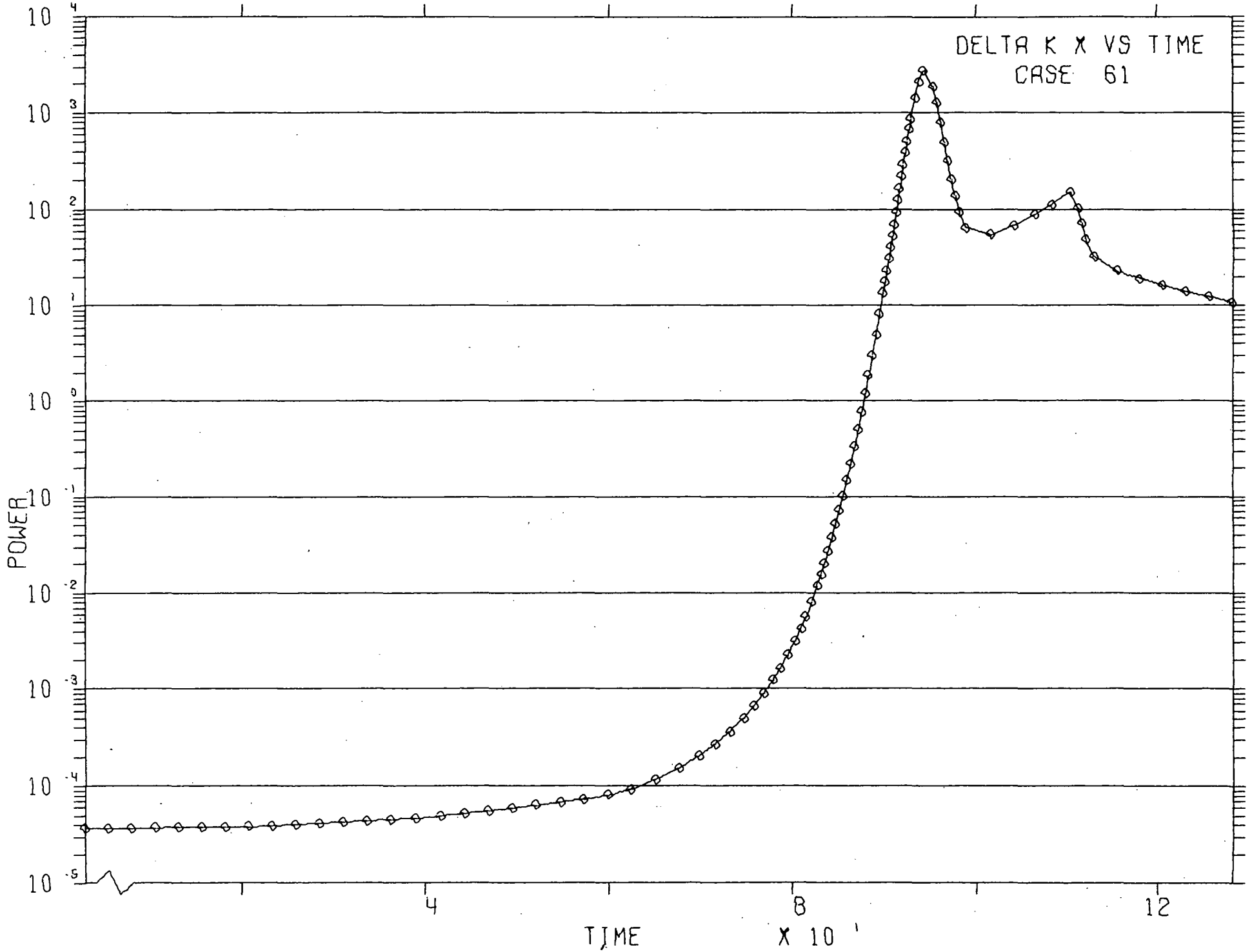
DELTA K X VS TIME
CASE 61
POWER
TIME
X 10
4
8
12

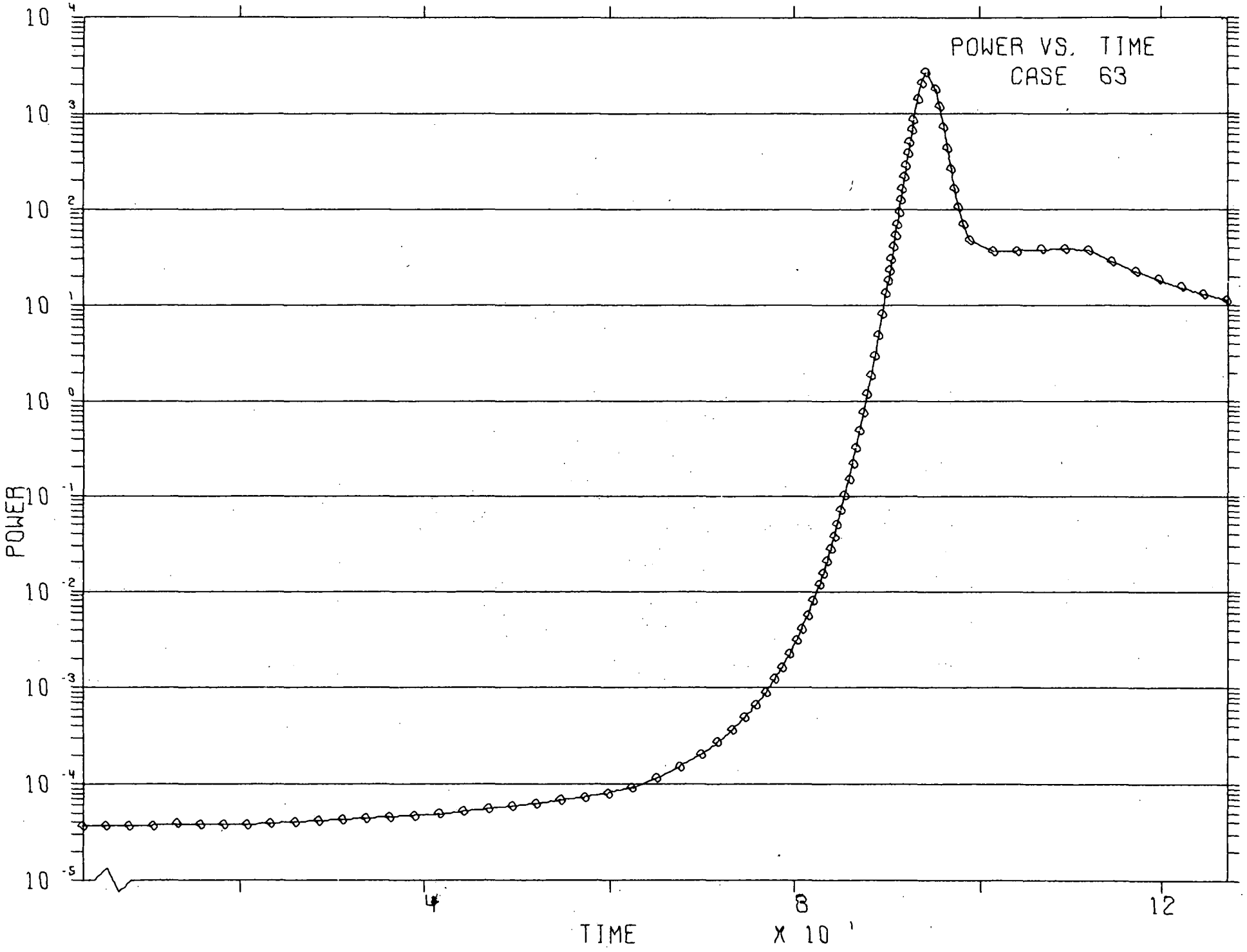

Figure 9

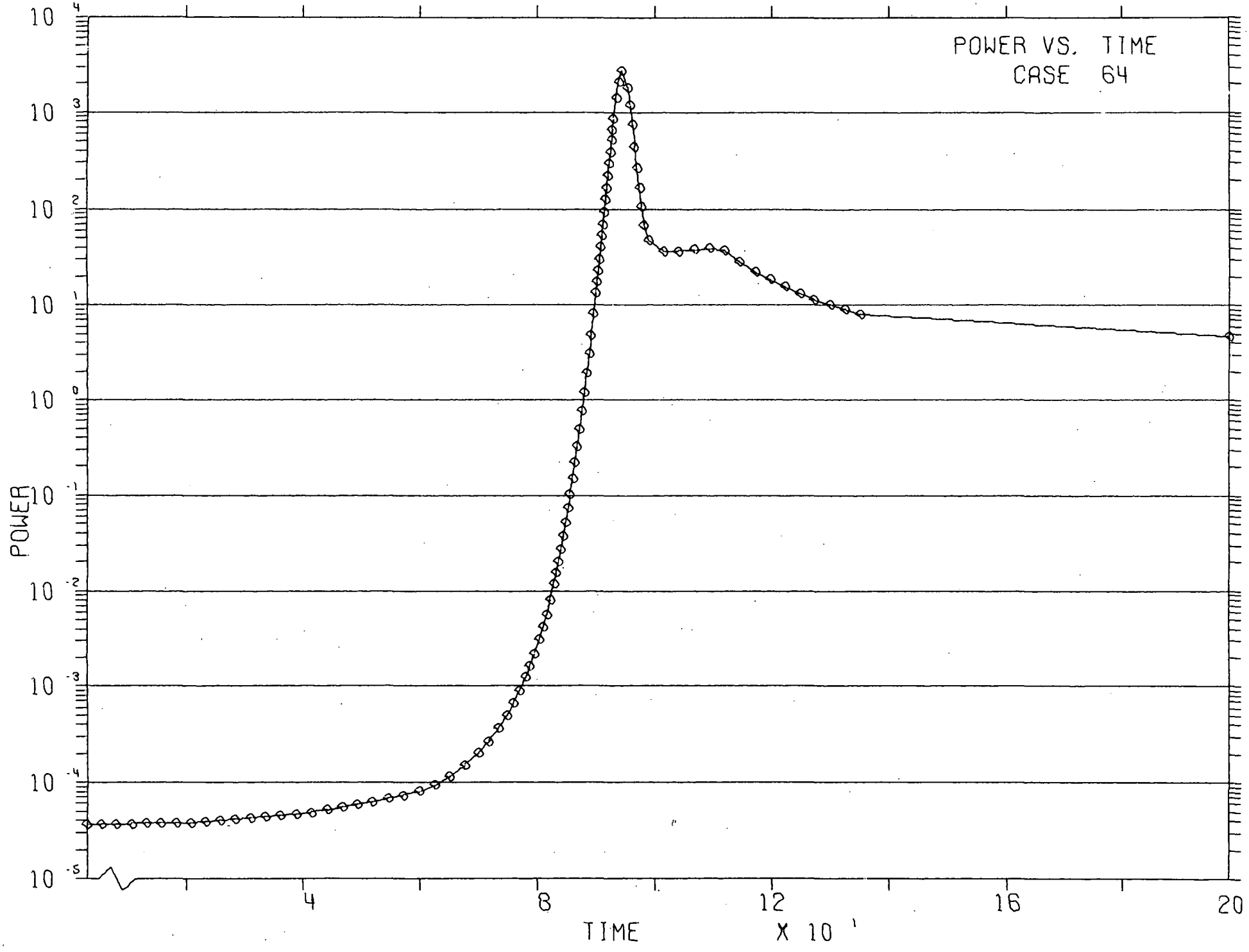
POWER VS. TIME
CASE 64
POWER
TIME
X 10 1
10 5
10 4
10 3
10 2
10 1
10 0
10 -1
10 -2
10 -3
10 -4
10 -5
4
8
12
16
20

Figure 10

the excursion. For large reactor systems which may potentially undergo super-prompt critical excursions, the integrity of the primary system would be threatened if a few percent of the fission energy were converted to mechanical energy. In a large boiling water reactor, the dominant factor which affects the energy conversion efficiency is the rate at which the thermal energy released in the nuclear burst may be transferred to the water. After the reactivity is inserted into the assembly, for excursions in which the assembly becomes super-prompt critical, there is a prompt power burst and, for UO_2 rod-type fuel, more than 90% of the nuclear energy released may remain stored in the fuel at the termination of the nuclear burst[11]. This stored energy is then ultimately released to the moderator and the remainder of the system at a rate which is primarily determined by the condition of the fuel rod. If the energy density in the fuel is low enough so that there is no loss of clad integrity, the relatively long heat transfer time constant of the fuel results in conduction of the heat out of the fuel over a period of several seconds, and this release rate poses no threat to the reactor primary system. With cladding failure, there is the potential for an increase in the transfer rate of stored energy out of the fuel, depending upon the degree and rate of fuel fragmentation and dispersal into the moderator.

At the bottom of the fuel failure scale is the so-called burnout phenomenon. This is caused by steam blanketing and ultimate melting of the clad. The fuel is then exposed to the moderator and fuel fragmentation may occur. This type of failure is characterized by a gradual fragmentation and dispersal. As the fuel enthalpy increases, internal pressure will be increased and the failure is then characterized by rapid fragmentation and dispersal, depending upon the high pressure energy available to accelerate the fuel particles into the moderator. Therefore, two thresholds of fuel enthalpy become important, the initial loss of clad integrity threshold which may result in system contamination, and the prompt dispersal threshold which may threaten the integrity of the primary system.

Calculational Model

An analytical fuel failure model has been developed to investigate the fuel failure phenomenon. Although this model incorporates idealizing assumptions and requires inputs which are not precisely known, it does provide a means of investigating the effects of the various phenomena and it can also be used to provide a measure of the sensitivity of the fuel failure thresholds to the various fuel design parameters.

As a result of the analytical studies, a position on fuel failure mechanisms, as summarized in Figures 11, 12, and 13, has been adopted.

Experimental Data

Because of the importance of the effects of fuel rod failures, a rather extensive literature search has been conducted. A summary of the published data available is presented in Figure 14. By far the most inclusive source of data is that from the ANL TREAT metal-water studies. There are two major differences between the characteristics of the TREAT tests and what one would expect in a large boiling water reactor, as indicated in Figure 15.

FUEL FAILURE MECHANISMS
APED POSITION

TWO BASIC TYPES OF FUEL FAILURE

I DELAYED FAILURE

WEAKENING AND ULTIMATELY MELTING OF CLAD DUE TO HEAT DECAY OUT OF HOT FUEL.

FAILURE DELAYED DUE TO LONG THERMAL TIME CONSTANT OF FUEL PINS.

II PROMPT FAILURE

CLAD BURST DUE TO EXCESSIVE INTERNAL PRESSURE.

Figure 11

I DELAYED FAILURE

A THRESHOLD FOR NO COOLANT FLOW ~170 CAL/GRAM

B NATURE OF FAILURE

GRADUAL FRAGMENTATION AND DISPERSAL OF FUEL INTO WATER

C CONSEQUENCES OF FAILURE

- MODEST PRESSURE RISE
- POSSIBLE LOCAL FUEL DAMAGE
- NO THREAT TO PRIMARY SYSTEM

Figure 12

II PROMPT FAILURE

A THRESHOLD (INDEPENDENT OF COOLANT FLOW) ~ 425 cal/gram

B NATURE OF FAILURE

PROMPT DISPERSAL OF FINELY FRAGMENTED FUEL INTO WATER

C CONSEQUENCES OF FAILURE

- HIGH PRESSURE RISE RATE
- THREAT TO PRIMARY SYSTEM INTEGRITY IF ENERGY CONTENT IS SUFFICIENT

Figure 13

FUEL FAILURE MECHANISMS
EXPERIMENTAL DATA

I. ANL TREAT TESTS
   COMPLETE RANGE OF
   FUEL ENTHALPY

II. SPERT-I INTEGRAL CORE TEST
   MAXIMUM FUEL ENTHALPY ~ 130 cal/gram

III. PULSTAR
   MAXIMUM FUEL ENTHALPY ~ 200 cal/gram

IV. GE-APO TREAT TESTS
   FUEL ENTHALPY ~ 270 cal/gram

Figure 14

I ANL TREAT TESTS

MAJOR DIFFERENCES BETWEEN TREAT TESTS AND BWR EXCURSIONS

(A) TIME SCALE

	ENERGY DEPOSITION cal/gram	MINIMUM PERIOD msec
TREAT	200-600	150-40
BWR	200-600	10-1

(B) COOLANT FLOW

TREAT - SMALL CAPSULE, NO FLOW

BWR - FORCED OR NATURAL CONVECTION

Figure 15

Figure 16 presents a summary of the final fuel particle size as a function of fission energy input into the fuel for single rods of UO_2 fuel[12][16]. This curve contains no time information, so very little can be said at this point concerning failure rate. However, the nature of the curve strongly implies three characteristic domains.

(1) Below ~ 200 calories per gram, no fragmentation of fuel occurs.

(2) Between ~ 200 and ~ 400 calories per gram is a transitional domain in which final fuel particle diameter is a strong function of energy input.

(3) Above ~ 400 calories per gram, the final fuel particle diameter is independent of energy input.

This curve very definitely indicates an initial failure threshold of approximately 200 calories per gram. This agrees very well with the analytical model prediction of approximately 170 calories per gram. The curve further implies that a change of failure mechanism occurs at approximately 400 calories per gram. If this is true, then it agrees very well with the prompt (internal pressure as opposed to clad melting for the lower thrshold) failure threshold prediction of the analytical model of approximately 425 calories per gram. If the prompt failure hypothesis is to be verified or invalidated, some time information is required.

The pressure rise rate in the test autoclave for most of the data in Figure 16 has been published in the ANL reports[12][13]. Figure 17 shows the superposition of the autoclave pressure rise rate on the previous curve. To emphasize the message of Figure 17, consider the two tests on zircaloy clad UO_2 pins with energy inputs of 280 and 450 calories per gram.

Input energy (cal/gm)	280	450
Final mean particle diameter (mils)	60	30
Pressure rise rate (psi/sec)	30	600

The ultimate degree of fuel fragmentation and dispersal of the two cases is not significantly different; however, the pressure rise rate in the higher energy test is increased by a factor of 20. This very strongly implies that the dispersion rate in the higher energy test was significantly higher than that of the lower energy. This leads to the logical conclusion that, although a high degree of fragmentation occurs for fuel in the 200 to 300 calories per gram range, the breakup and dispersal into the water is gradual and pressure rise rates are very modest. On the other hand, for fuel above the 400 calories per gram range, the breakup and dispersal is prompt and much larger pressure rise rates are probable. This agrees completely with the predictions of the analytical model. Unfortunately, no data is available between 300 and 400 calories per gram, so there is still some uncertainty as to the precise location of the prompt rupture threshold, if indeed it is sharp threshold. One might suspect that the statistical variations in test samples, variations in reactor period, and the interaction of the effects of clad weakening due to heat decay and pressure buildup due to fission gas and UO_2 vapor will result in a rather gradual threshold in the 300 to 450 calories per gram range.

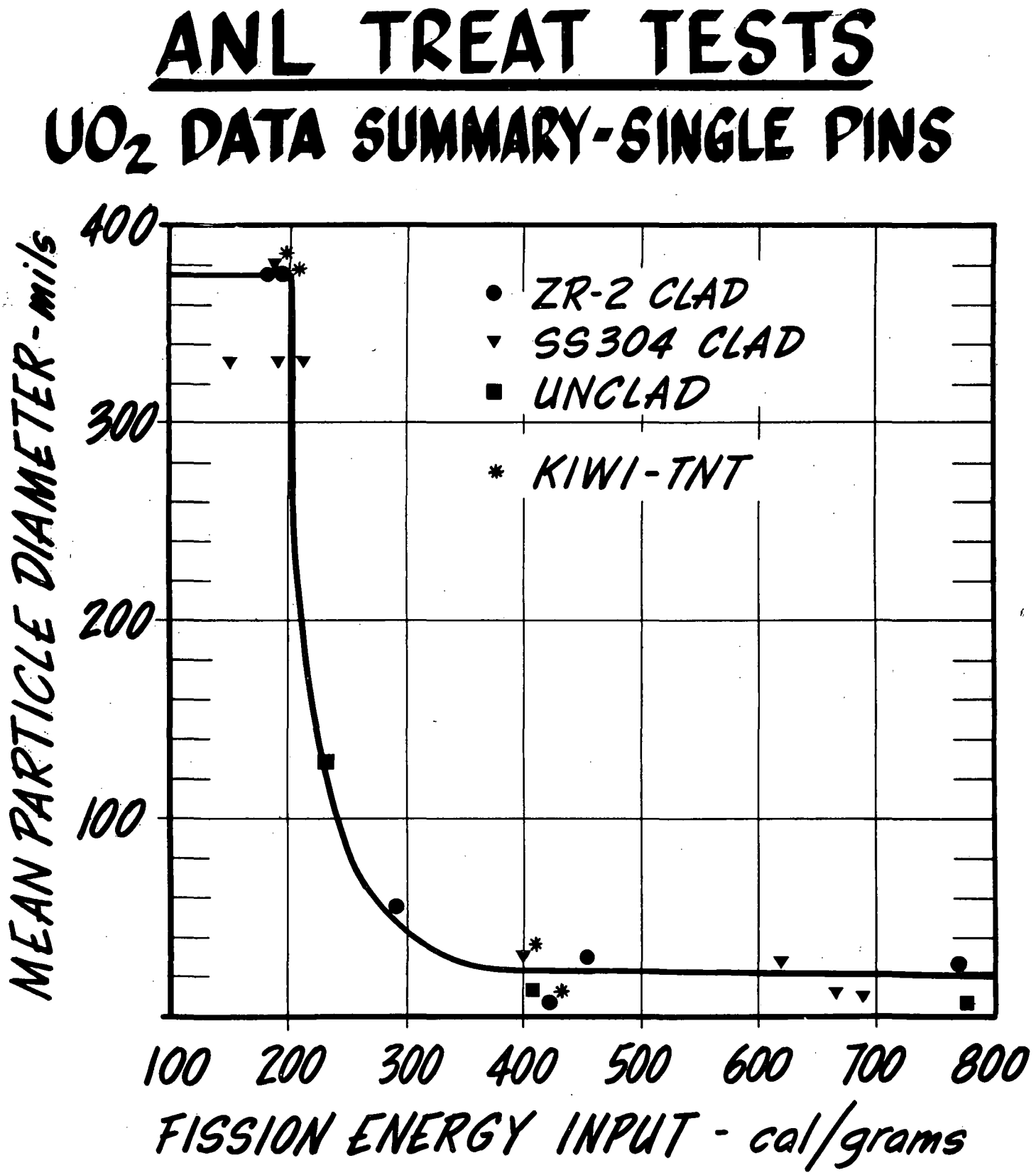
ANL TREAT TESTS
UO2 DATA SUMMARY-SINGLE PINS
MEAN PARTICLE DIAMETER-mils
400
300
200
100
ZR-2 CLAD
SS304 CLAD
UNCLAD
KIWI-TNT
100
200
300
400
500
600
700
800
FISSION ENERGY INPUT - cal/grams

Figure 16

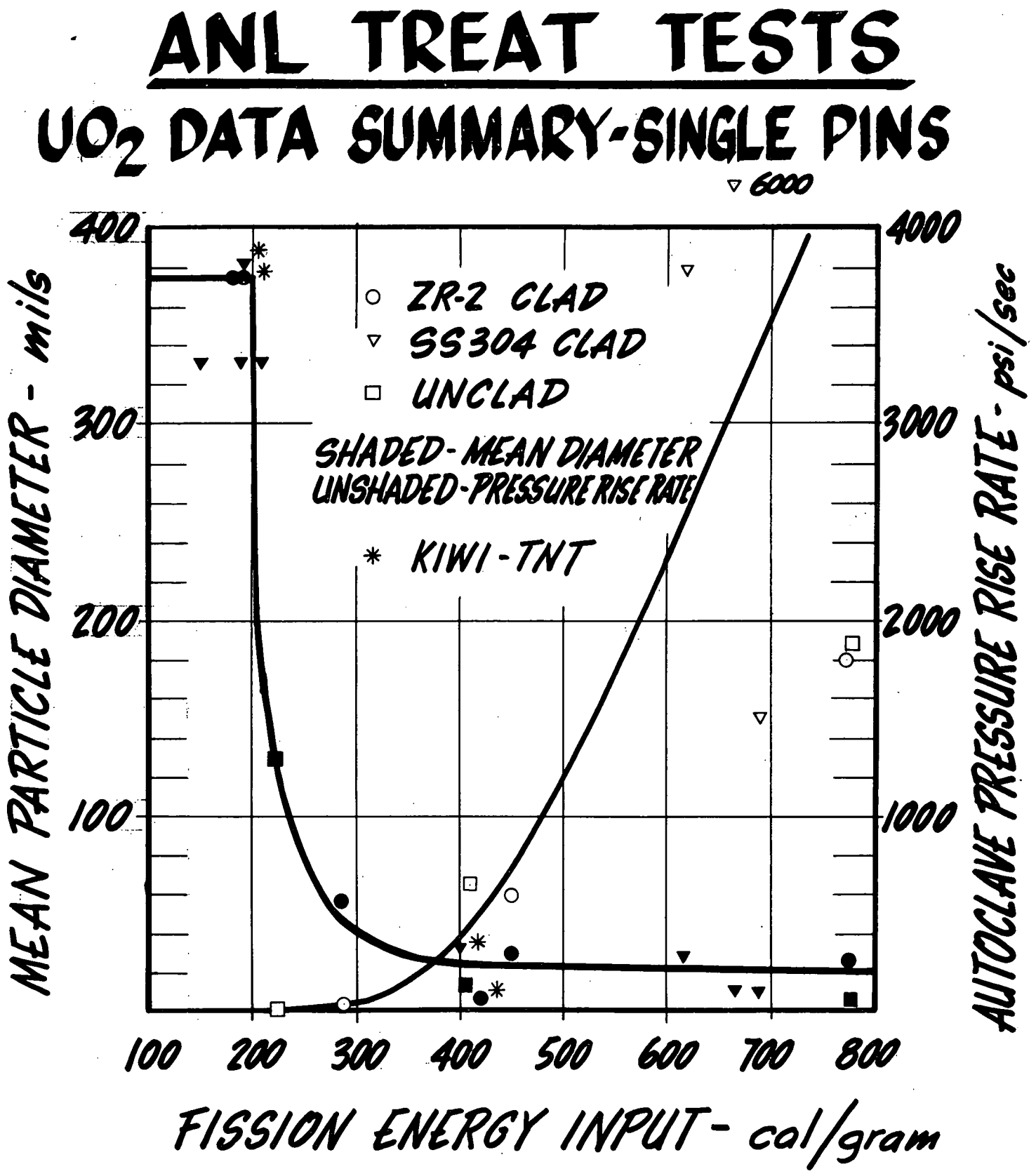
ANL TREAT TESTS
UO2 DATA SUMMARY-SINGLE PINS
▽ 6000
ZR-2 CLAD
SS304 CLAD
UNCLAD
SHADED-MEAN DIAMETER
UNSHADED-PRESSURE RISE RATE
KIWI-TNT
MEAN PARTICLE DIAMETER - mils
AUTOCLAVE PRESSURE RISE RATE - psi/sec
400
300
200
100
4000
3000
2000
1000
100 200 300 400 500 600 700 800
FISSION ENERGY INPUT - cal/gram

Figure 17

Nine fuel rod test[14] results are summarized in Figure 18. Very little detailed data has been reported on these tests, but the results are in accord with the previous analysis and data.

The fuel failures observed in the SPERT-1 oxide tests[8] are not typical of UO_2 pellet fuel in that this fuel was defective, unsintered powder fuel. Clad punctures, existing prior to the tests, had allowed the powder fuel to become saturated with water and high water vapor pressure caused premature failure of the fuel pins. This data is summarized in Figure 19.

The PULSTAR reactor is located in Buffalo, New York, and is a UO_2 pellet fueled test reactor capable of operating at very short periods. Figure 20 summarizes the effect on some test pins after ten successive power bursts, each of which brought the fuel to the incipient melting point[15]. This test series lends support to the assertion that the lower fuel failure threshold is not below approximately 200 calories per gram for short period excursions.

Figure 21 presents a data summary of the irradiated fuel tests carried out by the Advanced Products Operation of General Electric in the TREAT facility. These tests are the first in a series to determine the effects of the presence of fission products on fuel failure mechanisms during a rapid transient.

No information available at the present time would lead to a change in the current position on fuel failure mechanisms or damage thresholds.

ANL TREAT TESTS

NINE PIN BUNDLE

CLAD	ENTHALPY cal/gram	FUEL CONDITION	MAXIMUM PRESSURE RISE psi
ZR-2	250	INTACT	54
ZR-2	485	FRAGMENTED	304
SS-304	463	FRAGMENTED	223
SS-304	475	FRAGMENTED	110

"NO EXPLOSIVE PRESSURE RISES WERE OBSERVED"

Figure 18

SPERT-I

ΔK PERCENT	PEAK FUEL ENTHALPY cal/gm	FUEL ENTHALPY AT TIME OF BURST cal/gm	CONSEQUENCES
1.5	~84	—	NONE
1.9	~120	~40	RUPTURE OF WATER-LOGGED PINS
2.4	~130	~30	RUPTURE OF WATER-LOGGED PINS

Figure 19

PULSTAR

UO_2 PELLETS-6% ENRICHED-ZR-2 CLAD

TEN SUCCESSIVE POWER BURSTS

MINIMUM PERIOD – 2.83 ms

MAXIMUM FUEL ENTHALPY – ~200 CAL/GM

COOLANT FLOW – NATURAL CONVECTION

CONSEQUENCES

- FILM BOILING OCCURED
- FUEL PIN INTEGRITY MAINTAINED
- NO ABNORMAL PRESSURE RISE
- LOCAL CLAD BULGES

  1-6 % DIAMETRAL GROWTH

Figure 20

APO TREAT TESTS
SODIUM COOLED TO PREVENT CLAD MELTING

ENTHALPY cal/gram	EXPOSURE mwd/t	CONSQUENCES
~ 270	0	NO CLAD DEFORMATION
~ 270	7900	~1.2% CLAD STRAIN
~ 230	64,000	NO CLAD DEFORMATION

Figure 21

APPENDIX

This appendix compares the General Electric Doppler model to the models of Pettus and Hellstrand. The work of Pettus and Hellstrand is used for comparison because of all data reviewed it is considered to be the most carefully performed work directly applicable to the UO_2 fueled boiling water reactors.

The equations involved are summarized below:

Pettus

$$I = I_o [1 + \alpha (\sqrt{T} - \sqrt{T_o})]$$

$$I_o = 3.0 + 28.0 \sqrt{S/M}$$

$$\alpha = .0075 \text{ @ } S/M = .449$$

$$\alpha = .0063 \text{ @ } S/M = .206$$

Hellstrand

$$I = I_o [1 + \alpha (\sqrt{T} - \sqrt{T_o})]$$

$$I_o = 4.15 + 26.6 \sqrt{S/M}$$

$$\alpha = .0058 + .005 (S/M)$$

General Electric

$$I = I_o \exp [\alpha (\sqrt{T} - \sqrt{T_o})]$$

$$I_o = 30\sqrt{S/M + .077}$$

$$\alpha = .00696 - .000262 (M/S)$$

Figure A-1 shows the Doppler reactivity decrement as a function of fuel temperature for a typical BWR with fuel and moderator initially at 547°F. The General Electric curve is conservative relative to the others throughout the temperature range of the original data (below ~ 1800°F). At 5000°F the General Electric model is 5% less conservative than the Pettus model extrapolation but is about 5% more conservative than Hellstrand. However, the exponential temperature dependent form of the General Electric resonance integral equation is better justified theoretically than the simple square root dependence on temperature used by Pettus and Hellstrand.

Futhermore, high temperature Doppler measurements at Hanford[17] lend additional support to the exponential form. There is no significance, therefore, to the crossover of the General Electric extrapolation by the Pettus curve in Figure A-1.

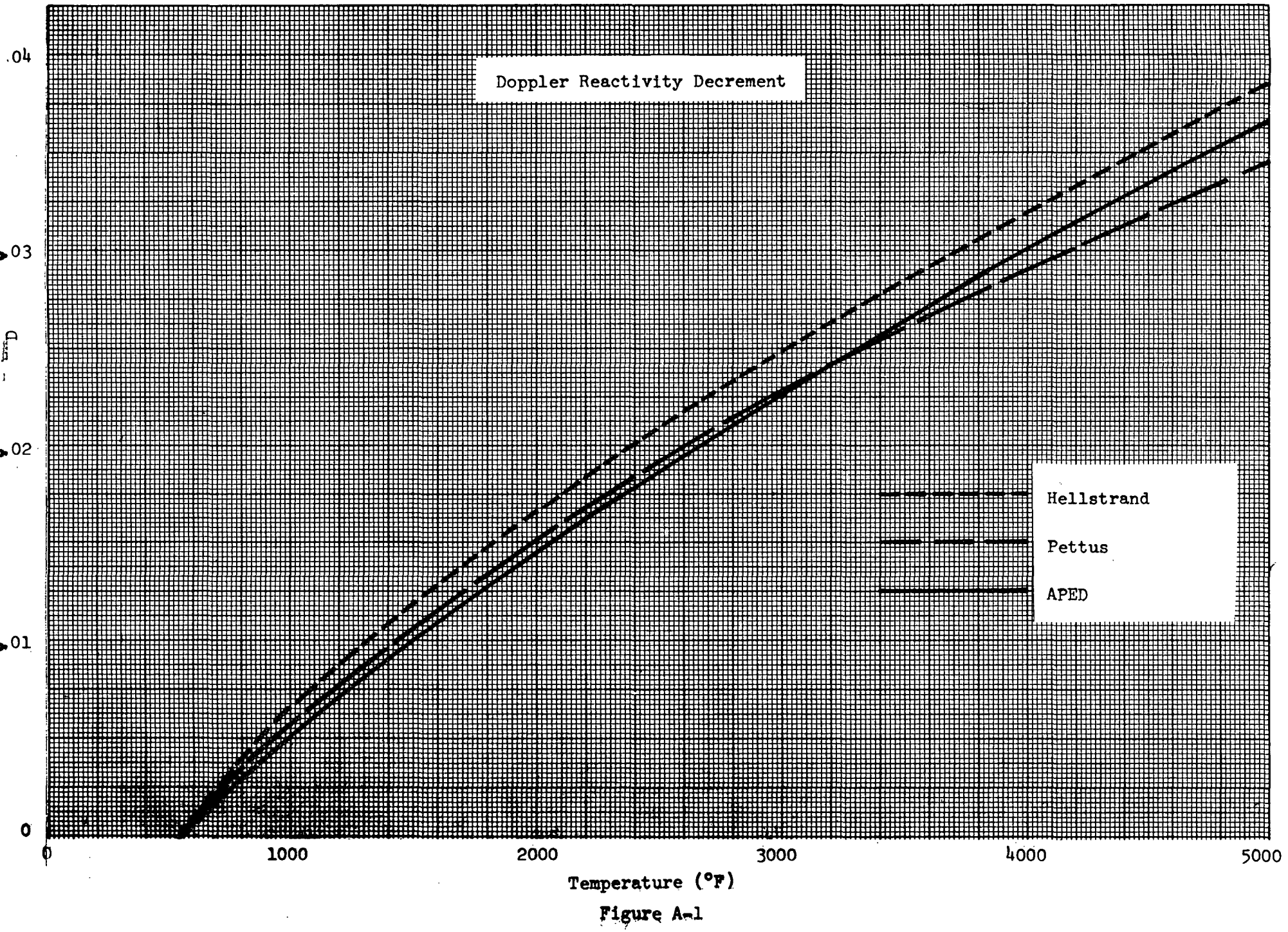
Doppler Reactivity Decrement
.04
.03
.02
.01
0
δk_{eff}
0
1000
2000
3000
4000
5000
Temperature (°F)
Hellstrand
Pettus
APED

Figure A-1

For the conditions included in Table I the Pettus and Hellstrand form of the Doppler used in equation (5) yields $\hat{H}$ = 211 cal/gm. The General Electric model, for the same, conditions predicts $\hat{H}$ = 220 cal/gm, or about a 5% more conservative value. Since the extrapolation to elevated temperatures using the General Electric model is the more theoretically sound, it is expected that this 5% conservatism will persist into the high temperature range.

REFERENCES

[1] WAPD-TM-416, "WIGLE - A Program for the Solution of the Two-Group Space-Time Diffusion Equations in Slab Geometry", W.R. Cadwell, et.al., January 1964.

[2] See Appendix for discussion of this equation.

[3] BAW-1244 "Resonance Absorption in U-238 Metal and Oxide Rods", W. G. Pettus, April 1962 (corrected February 1966).

[4] Hellstrand, E., et.al., "The Temperature Coefficient of the Resonance Integral for Uranium Metal and Oxide", N. S. and E. 8, p.497, December 1960.

[5] Hellstrand, E., "Measurements of the Effective Resonance Integral in Uranium Metal and Oxide in Different Geometries", Jrn. of Applied Physics, 28, December 1959.

[6] e.g., presentation on Metropolitan Siting and Related Programs by General Electric Co. to J. Lieberman, DRD, et.al., May 3, 1966.

[7] DNPS Unit 2, Plant Design and Analysis Report, Amendment 5, page 4-1.

[8] Grund, J. F., "Experimental Results of Potentially Destructive Reactivity Additions to an Oxide Core", IDO-17028, December 1964.

[9] Scott, R., Jr., Wasserman, A. A., and Schmitt, R. C., "Transient Tests of the Spert-1 Low-Enrichment UO_2 Core ", Data Summary Report IDO-16752, September 1963.

[10] Millstone Nuclear Power Station Design and Analysis Report, Amendment 3, page 6-1.

[11] A. N. Spano and J. E. Houghtaling, "Analysis of Fast Transient Reactivity Effects in the SPERT-1 Water-Moderated, UO_2- Fueled Core," IDO-17054 (May, 1965).

[12] L. Baker, Jr., and A. D. Tevebaugh, "Chemical Engineering Division Report, July-December, 1964, Section V - Reactor Safety," ANL-6925.

[13] L. Baker, Jr., and A. D. Tevebaugh, "Chemical Engineering Division Report, January-June, 1964, Section V - Reactor Safety," ANL-6900.

[14] R. M. Adams and A. Glassner, "Reactor Development Program Progress Report," ANL-7105 (October, 1965).

[15] J. MacPhee and R. F. Lumb, "Summary Report, PULSTAR Pulse Tests-II," Report No. WNY-020 (February, 1965).

[16] L. Baker, Jr., and A. D. Tevebaugh, "Chemical Engineering Division Summary Report, January-June, 1965, Section V - Reactor Safety," ANL-7055.

[17] HW-63766, PCTR Measurements of the EGCR Fuel Temperature Coefficient, F. C. Engesser, et.al., February 3, 1960.